Available online at www.sciencedirect.com
ScienceDirect
Chinese Journal of Natural Medicines 2021, **19**(3): 231-240
doi: 10.1016/S1875-5364(21)60025-0
Chinese Journal of Natural Medicines

•Research article•

Preparation and evaluation of a water-in-oil nanoemulsion drug delivery system loaded with salidroside

LIANG Chun-Xia[1, 2Δ], QI Dong-Li[1, 2Δ*], ZHANG Li-Na[1, 2], LU Peng[1, 2], LIU Zhi-Dong[1, 2*]

[1] *State Key Laboratory of Component-based Chinese Medicine, Tianjin University of Traditional Chinese Medicine, Tianjin 301617, China;*
[2] *Engineering Research Center of Modern Chinese Medicine Discovery and Preparation Technique, Ministry of Education, Tianjin University of Traditional Chinese Medicine, Tianjin 301617, China*

Available online 20 Mar., 2021

[ABSTRACT] Salidroside (SAL) is a phenolic substance with high solubility and low permeability, which make it easy to cause the efflux effect of P-glycoprotein and degradation of intestinal flora, resulting in lower bioavailability. The aim of this study was to develop and optimize a water-in-oil nanoemulsion of SAL (w/o SAL-N) to explore its suitability in oral drug delivery systems. In this work, SAL-N was successfully prepared by water titration method at K_m = 1 to construct the pseudo-ternary phase diagrams. Physical characterization including the average viscosity, pH, refractive index, particle size, PDI, TEM, DSC, the content of SAL, and stability study were performed. It was evaluated for drug release *in vitro* and pharmacokinetic studies *in vivo*. The optimized nanoemulsion formulation consisted of Labrafil M 1944CS (63%), Span-80/Tween-80/EtOH (27%) and 200 mg·mL^{-1} SAL solution (SAL-SOL) (10%). Low viscosity and suitable pH were expected for the nanoemulsion. The spherical morphology and nanoscale size of SAL-N enhanced the stability of the nanoemulsion system. *In vitro* drug release showed that SAL-N had a better controlled release property than SAL-SOL at earlier time points. The pharmacokinetic studies exhibited that SAL-N had significantly higher in $t_{1/2}$ (2.11-fold), $AUC_{0-48\ h}$ (1.75-fold) and $MRT_{0-48\ h}$ (2.63-fold) than SAL-SOL ($P < 0.01$). The w/o SAL-N prepared in this work can be effectively delivered *via* the oral route. It can be seen w/o nanoemulsion is a strategy for the drug with polyphenols to delay the release, enhance oral absorption and reduce metabolic rate.

[KEY WORDS] Salidroside; Water-in-oil nanoemulsion; Polyphenol; Drug release; Pharmacokinetics; Bioavailability
[CLC Number] R944 **[Document code]** A **[Article ID]** 2095-6975(2021)03-0231-10

Introduction

Salidroside (SAL) is a main biologically active ingredient from a well-known traditional Chinese medicine named Arctic Root (*Rhodiola rosea*) [1-2]. Recent studies confirmed that SAL has several pharmacological effects including antioxidant [3], anti-inflammatory [4], anti-stree [5-6], anti-fatigue [7], anti-cancer [8] and preventing acute mountain sickness etc [9-10]. Structurally, SAL is a phenolic substance formed by combining one molecule of tyrosol and one molecule of glucose. It belongs to the third category in the biopharmaceutical classification system (BCS) guidance with high solubility and low permeability, which makes it rapid released in the gastrointestinal tract. However, the efflux of P-glycoprotein in the intestinal mucosa and the influence of the intestinal flora reduce its oral absorption [11-12]. Polyphenols, such as SAL, have a wide range of pharmacological effects [13]. Therefore, according to the characteristics of these compounds, the appropriate formulations are essential to be designed to delay the drug release, reduce the metabolism rate and improve oral absorption to ensure the efficacy.

The current drug delivery systems for polyphenols are mainly nanoformulations, including solid lipid nanoparticles, liposomes, nanoemulsion and nanoemulsion. Nanoemulsion (N), a novel pharmaceutical formulation, is known to improve the drugs bioavailability after oral administration [14], which is a thermodynamically stable liquid system with particle sizes of 5 to 100 nm [15-16]. Recently, the high-value application of nanoemulsion in food and medicine has been

[Received on] 13-Apr.-2020
[Research funding] This work was supported by Tianjin City High School Science Technology Fund Planning Project (No. 2017KJ134).
[*]**Corresponding author]** E-mail: qidongli@tjutcm.edu.cn (QI Dong-Li); liuzhidong@tjutcm.edu.cn (LIU Zhi-Dong)
[Δ]These authors contributed equally to this work.
These authors have no conflict of interest to declare.

increasing due to a number of important advantages, such as sustained drug release, enhanced permeability, low side effects and prolonged efficacy [17-18]. Structurally, nanoemulsion are categorized into water-in-oil (w/o), oil-in-water (o/w) and bicontinuous nanoemulsions. The w/o nanoemulsion can encapsulate water-soluble drugs in the inner water phase, which enhanced transmembrane capacity, reduced the effusion effect of P-glycoprotein, improved the effect of sustained release, maintained the retention time of the drug in the body, and reduce metabolic rate [19-20]. Therefore, SAL was used as the model drug in this study to prepare w/o SAL-N in order to release the water-soluble drug slowly and achieve long-term treatment function.

The goal of this study was to prepare w/o SAL-N with non-ionic surfactants which are less toxic than others including apricot kernel oil PEG-6 esters (Labrafil M 1944CS), polysorbate 80 (Tween 80) and sorbitan monooleate (Span-80) [21]. Physical characterization, *in vitro* drug release assay, *in vivo* pharmacokinetic studies were conducted to explore its applicability of oral drug delivery system. We believed that the w/o nanoemulsion is a hopeful drug delivery for the drug with polyphenols to delay the release, enhance oral absorption and reduce metabolic rate.

Materials and Methods

Materials

Salidroside (mass fraction ≥ 92.14%) was gotten from Zelang Biotechnology Co., Ltd. (Nanjing, China). Reference of salidroside (purity > 98%) was procured from National Institute for the Control of Pharmaceutical and Biological Products (Beijing, China). Theophylline (IS, purity ≥ 98%) was procured from Zhongxin Pharmaceuticals (Tianjin, China). Soybean phospholipids (SP) was purchased from Taiwei Pharmaceuticals (Shanghai, China). Sorbitan monooleate (Span-80), polysorbate 80 (Tween-80) and oleic acid (OA) were supplied by Jingchun reagent (Shanghai, China). Paraffin liquid, glyceryl monolinoleate (Maisine CC), Propylene glycol monolaurate (Lauroglycol 90), propylene glycol monocaprylate (Capryol 90), polyglyceryl-3dioleate (Plurol® Oleique CC497), linoleoyl polyoxyl-6 glycerides (Labrafil M2125CS), apricot kernel oil PEG-6 esters (Labrafil M 1944CS) and medium-chain triglycerides (Labrafac™ Lipophile WL1349) were purchased from Gattefosse (St-Priest, France). The marketed Rhodiola injection (Sofren injection) (SAL-INJ) was obtained from Tonghua Yusheng Pharmaceuticals (CAS:1001150601, Jilin, China). Ultrapure water was prepared by a Milli-Q system (Merck Millipore, USA). All other chemical reagents used in this study were of analytical grade.

Animals

Male Sprague-Dawley (SD) rats (250−300 g) were obtained from the Laboratory Animal Center of Vital River [Animal Certificate No. SCXK (Beijing) 2016-0006, China]. The protocol of the experimental was approved by Institutional Animal Care and Use Committee of TJUTCM (Ethics Certificate No. TCM-LAEC20170041). All rats were housed in a room under constant temperature and permitted free access to food and drinking water.

Determination of n-octanol/water partition coefficient of SAL

Equal volumes of aqueous phases (a series of PBS solutions with pH 1.2, 2.5, 5.0, pure water, 6.8, and 7.6) and *n*-octanol were mixed 24 h at room temperature to obtain a saturated aqueous and oil phases. Subsequently, a known volume of aqueous phases containing the SAL was added to an equal volume of oil phase. The mixture was placed in a thermostated shaking incubator (SZCL-4B, Yuhua instrument, China), shaken at 37 °C for 24 h, and centrifuged at 4000 r·min^{-1} for 10 min. The concentration of SAL in the aqueous phase and oil phase was determined by the analysis system of high-performance liquid chromatography (HPLC) (LC-10AT, Shimadzu, Japan), respectively. The chromatographic separation of SAL was accomplished on a Diamonsil C_{18} (200 mm × 4.6 mm, 5 μm, DIKMA). The column temperature was 30 °C. A mobile phase composed of water (A) and acetonitrile (B) was used for chromatographic separation by gradient elution. The HPLC gradient schedule was set as follows, 0−10 min: 10%→20% B; 10−12 min: 20% B; 12−13 min: 20%→10% B; 13−15 min: 10% B. Symmetrical and efficient peaks were achieved at a flow rate of 1 mL·min^{-1}. The detection wavelength was 278 nm.

$$n\text{-octanol/water partition coefficient} = \frac{\text{Drug concentration in oil phase}}{\text{Drug concentration in aqueous phase}}$$

Formulation of SAL-N

The pseudoternary phase diagram of SAL-N was drawn by combining the self-emulsification method with the external energy supply method [22-23]. The suitable cosurfactant was selected by studying the correlative solubility of cosurfactant and surfactant. SAL-SOL was added into the mixture of different oil phases, surfactants, and co-surfactants. The suitable surfactant, oil phase and the ratio of surfactant to cosurfactant (K_m) were selected to study whether the mixture can incorporate more water or not.

The prepation of SAL-N was using high-pressure homogenization (HPH) (AH100D, ATS, China). The temperature was maintained at 50 °C, Labrafil M 1944CS (63%), Span-80/Tween-80/EtOH (K_m = 1) (27%) and SAL-SOL (200 mg·mL^{-1}) (10%) (*W*/*W*/*W*) were added into the beaker mixing thoroughly, and then dispersed uniformly for 5 min by using the instrument of high-speed dispersion (FLUKE, Shanghai, China). The mixture was homogenized for 5 cycles at the 1.1 × 10^3 bar by the HPH to obtain the homogenized and transparent SAL-N.

Characterization of SAL-N

Determination of type

The type of SAL-N was identified by the dyeing method [24]. Sudan red (an oil-soluble dye) and Methylene blue (a

water-soluble dye) was added into two penicillin bottles of SAL-N to observe the diffusion of the two dyes, respectively.

Determination of viscosity

The viscosity of SAL-N were measured at room temperature (25 ± 1) °C following the adjustment the zero point of the DV-III rheometer (Brookfield, USA).

Determination of pH

The pH of SAL-N were assessed at room temperature (25 ± 1) °C following the calibration of the pH meter (Mettler Toledo, Switzerland) with standard liquids of pH 4.01, 6.86 and 9.18.

Determination of refractive index

The refractive index of SAL-N relative to air was measured at 589.1 nm by the WAY-2S Abbe refractometer (Shenguang Instrument, China) at ambient temperature. The refractometer should be calibrated with water before the measurement.

Measurement of the particle size (Z-average) and PDI

A volume of 1 mL of SAL-N was added into the particle size vessel, then the Z-average and PDI were determined by the Zetasizer (Malvern Nano ZS, UK) at room temperature (25 ± 1 °C).

Determination of morphology

A drop of SAL-N was taken on copper grids, and stained with 1% phosphotungstic acid solution to observe the morphology of the SAL-N by transmission electron microscopy (TEM, JEM-1200EX, Japan).

Determination of differential scanning calorimeter (DSC)

DSC measurements of water, SAL-SOL, physical mixture, formulation lacking SAL and SAL-N were determined in a cooling mode using a DSC Q200 instrument (TA Instruments, USA). Accurately weigh approximately 10 mg of the sample into an aluminum hermetic pan and sealed with the lid quickly. A blank aluminum pan was used as reference. Nitrogen gas at a flow rate of 50 mL·min^{-1} was used as the purge gas. The sample was cooled to −80 °C at a cooling rate of 10 °C·min^{-1}, hold for 1 min, heated to 25 °C at a rate of 10 °C·min^{-1}.

Determination of SAL concent

A volume of 0.2 mL of SAL-N was added into volumetric flask (50 mL), then diluted with methanol to as a sample solution. The concentration of SAL was determined by HPLC system (LC-10AT, Shimadzu, Japan).

Stability study

The stability of SAL-N was evaluated by appearance, centrifugation, particle size, viscosity, pH, refractive index and the content of SAL at ambient temperature up to 15 d.

In vitro drug release study

The release curve of SAL-N was assessed by making use of the dialysis bag (cut-off 7 kDa, Milipore, USA) diffusion technique using dissolution apparatus (DT-820, ERWEKA, Germany) [25]. 200 mL of PBS (pH 6.8 buffer) was used as the dissolution medium. 2 mL SAL-SOL and SAL-N were pipetted into the dialysis bag (Millipore USA), respectively. Under the condition of temperature was controlled at 37 ± 0.5 °C and the stirring rate was sustained at 100 r·min^{-1}. 2 mL of the sample was collected at 0.083, 0.167, 0.25, 0.5, 1, 2, 3, 4, 6 h. At the same moment, the fresh dissolution medium with an equal volume was added. The withdrawn samples were assayed by HPLC (LC-10AT, Shimadzu, Japan) after filtration with Millipore filter (0.45 μm).

Pharmacokinetic study

UPLC-MS/MS conditions

The analysis was tested by a UPLC-MS/MS system composed of UPLC system (an Agilent series 1290) and triple quadrupole mass spectrometer (an Agilent series 6460) (Agilent Technologies, USA). The chromatographic separation of SAL and IS was accomplished on an Acquity BEH UPLC C_{18} column (2.1 mm × 50 mm, 1.7 μm, Waters, USA). The column temperature was 30 °C. The temperature of autosampler was 4 °C. A mobile phase composed of water (A) and acetonitrile (B) was used by gradient elution. The UPLC gradient schedule was set as follows, 0.0−1.0 min: 10%→15% B; 1.0−2.5 min: 15%→20% B; 2.5−3.0 min: 20% B; 3.0−3.5 min: 20%→80% B; 3.5−4.5 min: 80% B; 4.5−5.0 min: 80%→10% B; 5.0−6.0 min: 10% B. Symmetrical and efficient peaks were achieved at a flow rate of 0.2 mL·min^{-1}. Electrospray negative ionization (ESI) was used to detect the SAL of plasma samples in the single ion monitoring mode (SIM). The monitored ion of salidroside and IS were *m/z* 299 and 180.1, respectively. The gas flow rate was 11 L·min^{-1}. The gas temperature was 350 °C. The fragmentor voltage was 100 V.

Preparation of stock solutions

The stock solution of SAL and IS was prepared in acetonitrile at a concentration of 100 μg·mL^{-1}, respectively. All the stock solutions were stored at 4 °C before use.

Preparation of plasma samples

100 μL plasma sample was added into a 1.5 mL Eppendorf tube, then 500 μL IS-containing acetonitrile solution (1000 ng·mL^{-1}) was added. Each sample was mixed in a vortex for 3 min and centrifuged at 12 000 r·min^{-1} for 10 min. 450 μL of the supernatant was dried with N_2. The remnant was dissolved with 20% acetonitrile and the resulting solution was mixed in a vortex for 3 min then centrifuged at 12 000 r·min^{-1} for 10 min. And 3 μL supernatant was injected into the UPLC-MS/MS system for assay.

Method validation

Under the guidelines of the China Food and Drug Administration (CFDA), we validated its specificity, linearity, precision, matrix effect, recovery and stability of the analytical method.

Based on the preparation of plasma samples, the plasma consisting of reference substance of SAL and IS, the blank plasma, and the plasma consisting of mixed reference solution were analyzed for the specificity. Construction of calibration curves were performed by diluting stock solutions to the concentration 5−20 000 ng·mL^{-1} for SAL to validate linearity of the method. Subsequently, linear regression equa-

tion analysis was performed with $1/X$ as a weighting factor. The precision of intra-day and inter-day were analyzed by the relative standard deviations (RSD) of the three concentration levels (50, 1000 and 16 000 ng·mL^{-1}) on the same day and three days in a row, respectively. The extraction recoveries of SAL were reckoned by contrasting the peak area proportion of SAL obtained from QC samples with those attained from the analytes which were dissolved in the supernatant of the preparation of blank plasma. The matrix effects of SAL were assessed by contrasting the peak areas aquired from blank plasma with those achieved from reference solutions at three QC levels. The stability study involved the stability of the analyte stored at 4 °C for 24 h in the autosampler and at −20 °C to room temperature for after three freeze-thaw cycles.

Pharmacokinetic study of SAL in SD rats

The SD rats were assigned into three groups (n = 6) and restricted access to food overnight but were freely supplied for water. SAL-SOL and SAL-N were administered at a dose of 100 mg·kg^{-1} by gavage. And the SAL-INJ was administered by tail vein injection at a dose of 15 mg·kg^{-1}. Then, plasma samples taken from orbital veins were collected into eppendorf tubes at 0.083, 0.25, 0.5, 0.75, 1, 1.5, 2, 3, 4, 6, 8, 10, 12, 24 and 48 h. After centrifugation at 4000 r·min^{-1} for 10 min. 100 μL of the supernatant was taken into another eppendorf tube and store at −20 °C before analysis.

Statistical analysis

All results were expressed as the mean ± standard deviation (SD) of at least three experiments in this work. Statistical analysis was accomplished by SPSS-22.0 software, and T-test was using to assay the difference between groups, $P < 0.05$ showing the significant difference, while $P < 0.01$ showing the extremely significant difference.

Results and Discussion

Determination of n-octanol/water partition coefficient of SAL

The n-octanol/water partition coefficient is closely related to the absorption of the drug in the gastrointestinal tract. It has been reported that the drug have higher membrane permeability when log P values ranging from 0 to 3 [26]. As shown in Table 1, SAL exhibits low lipophilicity (log P < 0 in different PBS), which shows that SAL is not easily absorbed from the intestinal mucosa after oral administration.

Table 1 n-Octanol/water partition coefficient (log$P$) of SAL in different media (mean ± SD, $n \geq 3$)

Media	log$P$
pH 1.2	−1.245 ± 0.004
pH 2.5	−1.194 ± 0.004
pH 5	−1.140 ± 0.006
pure water	−1.233 ± 0.006
pH 6.8	−1.176 ± 0.003
pH 7.6	−1.326 ± 0.006

Formulation of SAL-N

In the present study, the SAL-N was perfectly developed by high-pressure homogenization. In the pre-prescription screening, ethanol (EtOH) was known to have excellent miscibility and fluidity when it was mixture with variety of surfactants [27-29]. It was selected as the cosurfactant of SAL-N. The mixture of emulsifiers (W/W, 1 ∶ 1) showed that Span-80/Tween-80/EtOH can incorporate more water. It was mixed with different oil phases (Castor oil, soybean oil, Maiisine CC, liquid paraffin, LabrafacTM Lipophile WL1349, Labrafil M 1944CS, oleic acid, ethyl oleate), and then the product has blended with water. Fig. 1 showed the pseudoternary phase diagram drawn. The area of the nanoemulsion region was larger when Labrafil M 1944CS or OA as the oil phase. There was no obvious effect on the area of the nanoemulsion when Labrafil M 1944CS or oleic acid was used as oil phase after adding the drug. The results were showed in Fig. 2.

Compare to oleic acid, Labrafil M 1944CS requires less amount of surfactant with a larger area. And Labrafil M 1944CS was developed as a nonionic surfactant to minimize toxicity of nanoemulsion [21, 30]. Therefore, Labrafil M 1944CS was finally determined as the oil phase. The area of nanoemulsion was gradually increasing as the K_m increases. However, there is no significant change in the area when K_m is greater than one.

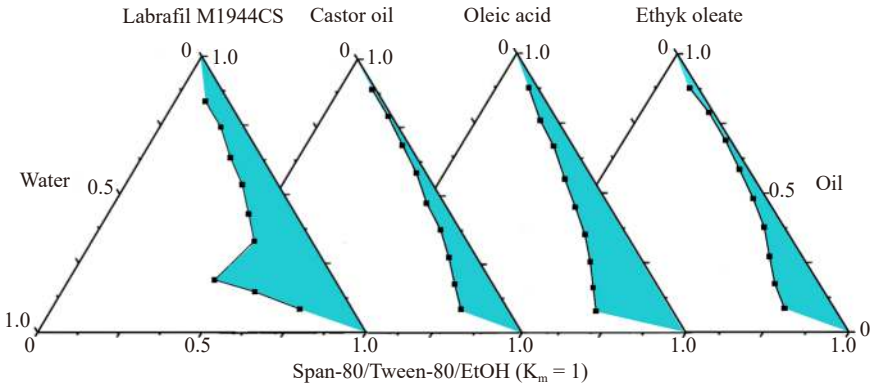

Fig. 1 Pseudoternary phase diagrams of different oil phases (The color part represents the nanoemulsion area)

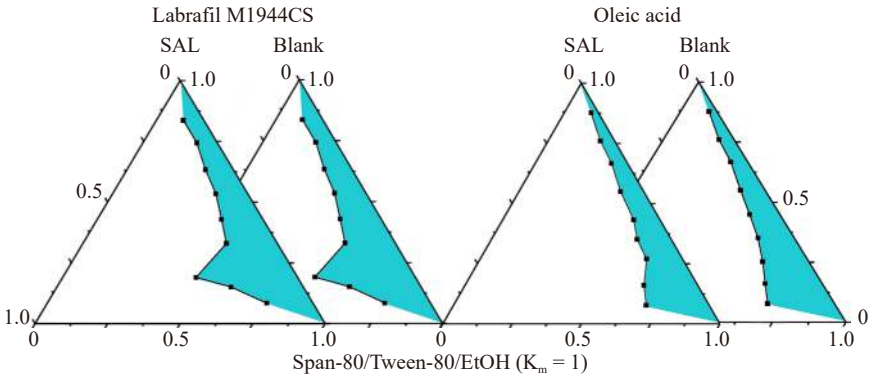

Fig. 2 The changes in Pseudoternary phase diagrams after the incorporation of the drug (The color part represents the nanoemulsion area)

Characterization of SAL-N

Determination of type

The physical characterization of nanoemulsion were a significant index to consider the practical applications. The results of dyeing experiments demonstated the group Methylene bluethe's diffusion rate in the SAL-N was slower than that of group Sudan red. The SAL-N belonged to w/o preparation, because methylene blue was observed in the internal phase and Sudan red in the external phase.

Determination of viscosity

The average viscosity of SAL-N was 80.37 ± 0.12 cPa·s, Low viscosity was expected for the nanoemulsion [31-32].

Determination of pH

Safety and stability of formulated nanoemulsion are affected by the pH value [33]. The pH of SAL-N was 5.68 ± 0.05, The suitable pH was expected for the nanoemulsion.

Determination of refractive index

The refractive index of SAL-N was 1.47 ± 0.01, which was closed to the water, indicating that the SAL-N were clear and transparent.

Measurement of the particle size (Z-average) and PDI

The *Z*-average and PDI of SAL-N were 32.51 ± 0.21 and 0.32 ± 0.00 nm, respectively. The nanoscale size could be due to its high content of the mixture of emulsifiers Span-80/Tween-80/EtOH. Fig. 3 shows the particle size distribution by intensity was narrower, which enhanced the stability for the nanoemulsion system by resist gravitational separation [22]. The smaller value of PDI indicated that the SAL-N was monodisperse [27].

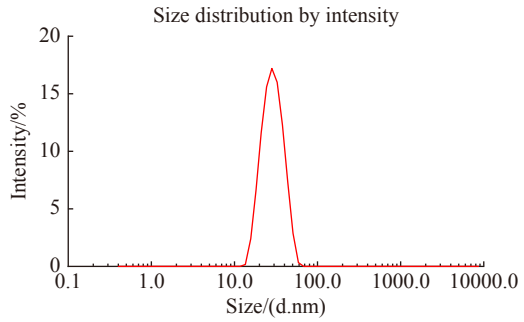

Fig. 3 The size distribution of SAL-N

Determination of morphology

The TEM images of the SAL-N was shown in Fig. 4. SAL-N appeared spherical morphology with a particle size smaller than 50 nm, which was consistent with the results obtained from the particle size analyzer.

Determination of differential scanning calorimeter (DSC)

Thermal behavior of water is used to understand the structure of nanoemulsion. The DSC curves for the different samples are shown in Fig. 5. Water (Fig. 5A) and SAL-SOL (Fig. 5B) showed sharp endothermic peaks at −10.95 and −13.85 °C, respectively, due to the freezing temperature of cold water [34]. Physical mixture (Fig. 5C) did not show endothermic peaks at the same position as water due to partial miscibility of water with surfactants and co-surfactants [35].

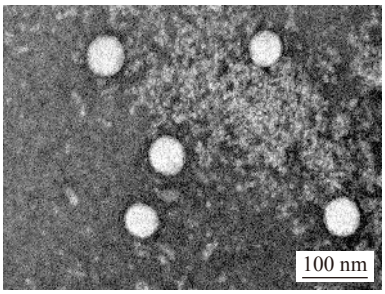

Fig. 4 The TEM images of the SAL-N

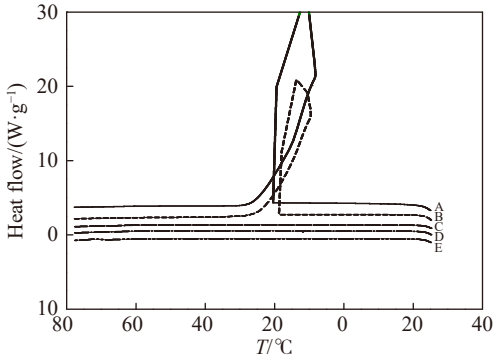

Fig. 5 DSC curves of (A) water, (B) SAL-SOL, (C) physical mixture, (D) formulation lacking SAL and (E) SAL-N

Formulation lacking SAL (Fig. 5D) and SAL-N (Fig. 5E) did not show endothermic peaks at the same position as water because water is encapsulated in the w/o nanoemulsion [36].

Determination of SAL concent

The drug concentration of SAL-N was 12.12 ± 0.33 mg·mL^{-1}.

Stability study

SAL-N did not show any phase separation, turbidity and precipitation after centrifugation at 12 000 r·min^{-1} for 10 min. Meanwhile, there was no significant difference in appearance, particle size, viscosity, pH, refractive index and the content of SAL at room temperature for 0, 7 and 15 days (Fig. 6), which proved that the SAL-N had a good physical stability.

In vitro drug release study

The release curves of SAL-N and SAL-SOL were displayed in Fig. 7. The dissolution rate of SAL in PBS (pH 6.8 buffer) was quite high due to the strong hydrophilicity. 100% of SAL was released from SAL-SOL and SAL-N within 2 h and 4 h, respectively. SAL-N had a better sustained release property at the early time points, indicating that SAL-N increased the fat solubility of the drug in the intestine because large proportion of the SAL were dissolved in the water phase and covered in the oil phase [21, 37]. This indicates that the oil and surfactant in the SAL-N can delay drug release within 4 h. But it could not accurately simulate what happens of SAL *in vivo* as a result of the existence of various different conditions such as enzymes, biological conditions, and drug carriers [38].

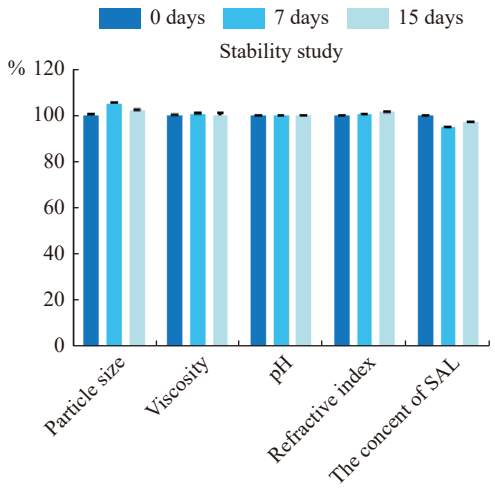

Fig. 6 The stability study of SAL-N

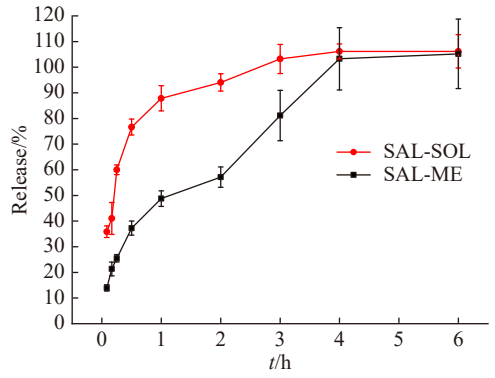

Fig. 7 *In vitro* release profiles of SAL from SAL-N and SAL-SOL (Each point represented as mean ± SD, *n* = 3)

Pharmacokinetic study of SAL-N in rat

Method validation

As showed in Fig. 8, the results show that the blank plasma doesn't interfere with the determination of salidroside and IS. Table 2 presented including calibration curve, linear range and correlation coefficient for the analytes. The correlation coefficients was more than 0.99 indicated the calibration curve revealed acceptable linearity. Table 3 showed the precision including intra-day and inter-day of the method, which were < 6.88% and < 4.47%, respectively. Table 4 showed the recovery of extraction recoveries and method recoveries were 90.16%−95.65% and 101.92%−106.36% for SAL at three QC levels, respectively. Area ratios of matrix effects were between 87.37% and 93.82%, showing that matrix effects could not be ignored. The results of stability were summarized in Table 5, indicating that SAL had no significant degradation at the condition of autosampler for 24 h and three freeze-thaw cycles.

Pharmacokinetic study

The plasma concentration of drug-time curves of the SAL-SOL, SAL-N and SAL-INJ were exhibited in Fig. 9. No significant difference in C_{max} was observed between SAL-SOL and SAL-N group. Compared with SAL-SOL, there was a double peak appearing after oral administration of SAL-N in rats. It was reported that there were several factors which caused the incidence of the double peak phenomenon, including enterohepatic recirculation, delayed gastric emptying, drug-drug interaction, and variability of absorption [39-41]. In this work, enterohepatic recirculation and delayed gastric emptying may be the primary reason for the double peak of SAL-N.

The relevant pharmacokinetics parameters were showed in Table 6. The $t_{1/2}$ of SAL-INJ was (0.083 ± 0.00) h, which exhibited faster elimination characteristics. Compared with SAL-SOL (3.82 ± 1.50 h), the $t_{1/2}$ of SAL-N was (8.06 ± 5.24) h. In addition, the MRT of SAL-SOL group was (2.34 ± 0.59) h, the MRT of SAL-N group was (6.15 ± 1.04) h, which represented 2.63-fold than that of SAL-SOL indicating that SAL-N significantly prolonged the residence time of the drug and reduced metabolic rate. The $AUC_{0\to t}$ of SAL-SOL group was (23.03 ± 4.78) h·μg·mL^{-1}. The $AUC_{0\to t}$ of SAL-N group was (40.32 ± 4.95) h·μg·mL^{-1}, which represented 1.75-fold than that of SAL-SOL, indicating SAL-N significantly enhanced the oral bioavailability of SAL.

There are several possible reasons for improved oral higher bioavailability of SAL-N. During the nanoemulsion formation, a greater proportion of salidroside is encapsulated

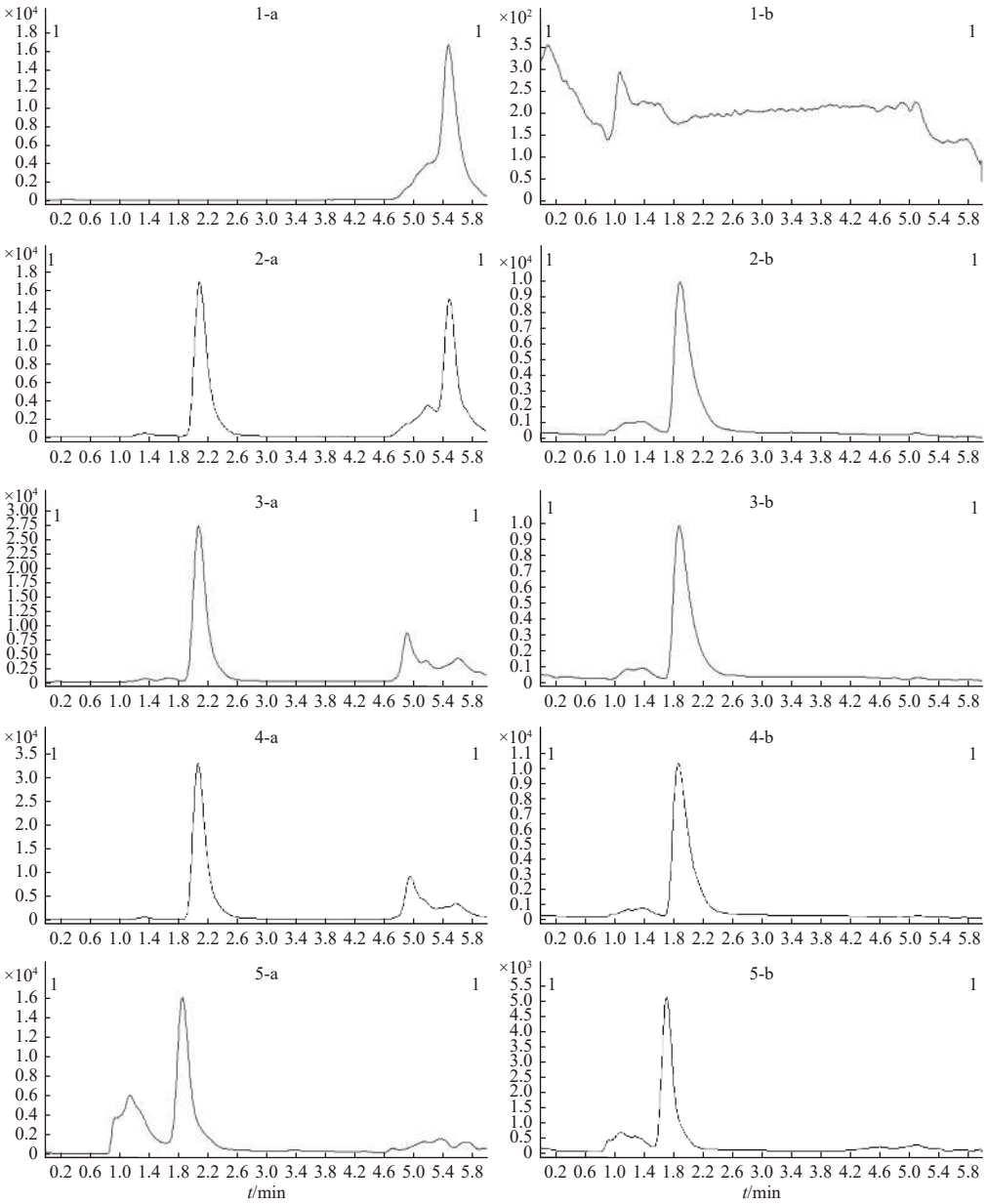

Fig. 8 Chromatograms of plasma samples (1-blank plasma; 2-standard plasma; 3-plasma sample of SAL-N; 4-plasma sample of SAL-SOL; 5-plasma sample of SAL-INJ; a-salidroside; b-IS)

Table 2 Linearity for assay of SAL in rat plasma

Analyte	Calibration curves	Linear ranges (ng·mL^{-1})	R^2	weight
SAL	$Y = 2.77 \times 10^{-4} X + 3.5 \times 10^{-3}$	5−20 000	0.9989	$1/X$

Table 3 Precision for assay of SAL in rat plasma (mean ± SD, $n \geq 6$)

Analyte	c/(ng·mL^{-1})	Precision			
		Intra-day precision		Inter-day precision	
		Measured	RSD (%)	Measured	RSD (%)
SAL	50	53.62 ± 3.19	5.95	50.50 ± 1.25	2.38
	1000	1074.00 ± 73.95	6.88	957.23 ± 42.74	4.47
	16 000	16 533.85 ± 245.94	1.57	14 181.23 ± 73.93	0.52

Table 4 Matrix Effects, extraction recovery and method recovery (mean ± SD, $n \geq 6$)

Analyte	c/(ng·mL^{-1})	Matrix effects		Extraction recovery		Method recovery	
		Average (%)	RSD (%)	Average (%)	RSD (%)	Average (%)	RSD (%)
SAL	50	93.82 ± 5.85	6.23	90.16 ± 3.87	4.29	101.92 ± 1.49	1.47
	1000	92.34 ± 3.55	3.85	91.04 ± 5.65	6.20	106.36 ± 2.17	2.55
	16 000	87.37 ± 1.06	1.21	95.65 ± 3.17	3.31	103.71 ± 1.56	1.49

Table 5 Stability for assay of SAL in rat plasma (mean ± SD, $n \geq 6$)

Analyte	c/(ng·mL^{-1})	Stability			
		Autosampler for 24 h		Three freeze-thaw cycles	
		Measured	RSD (%)	Measured	RSD (%)
SAL	50	55.10 ± 0.16	1.19	59.12 ± 0.70	1.18
	1000	1048.51 ± 37.91	3.62	1146.91 ± 45.83	4.00
	16 000	16 348.35 ± 191.00	1.17	16 486.84 ± 141.10	0.86

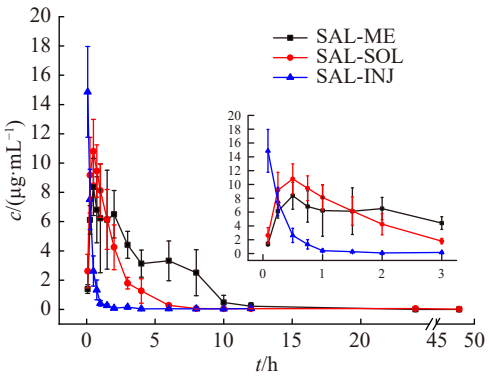

Fig. 9 Plasma concentration-time profiles of salidroside after oral administration of SAL-SOL and SAL-N and intravenous injection of SAL-INJ (mean ± SD, $n = 6$)

Table 6 Pharmacokinetics parameters of salidroside after oral administration of SAL-SOL and SAL-N and intravenous injection of SAL-INJ (mean ± SD, $n \geq 6$)

Parameters	SAL-SOL	SAL-N	SAL-INJ
t_{max}/h	0.50 ± 0.00	0.58 ± 0.20	0.083 ± 0.00
$t_{1/2}$/h	3.82 ± 1.50	8.06 ± 5.24*	0.54 ± 0.51
c_{max}/(μg·mL^{-1})	10.80 ± 2.18	9.31 ± 3.01	14.86 ± 3.10
AUC_{0-t}/(h·μg·mL^{-1})	23.03 ± 4.78	40.32 ± 4.95**	5.41 ± 0.56
Vz/F (L·g^{-1})	130.03 ± 60.44	93.92 ± 47.64	2.58 ± 2.73
CL/F/(L·h^{-1}·g^{-1})	12.23 ± 2.22	16.61 ± 4.50	3.02 ± 0.43
MRT/h	2.34 ± 0.59	6.15 ± 1.04**	0.30 ± 0.16

$^{*}P < 0.05$, $^{**}P < 0.01$ *vs* SAL-SOL

by the oil phase, which not only reduced enzymatic degradation but also delayed the *in vivo* metabolism [42]. The nanoscale size of SAL-N not only increase the ratio of surface area to volume for salidroside absorption but prolong interaction time on the gastrointestinal tract so that the oral bioavailability was improved [43-44].

Conclusion

In this study, the w/o SAL-N was efficiently prepared and characterized. The nanoscale size of SAL-N enhanced the stability of the nanoemulsion system. In comparison with SAL-SOL, SAL-N exhibited a better sustained drug release property. Furthermore, the pharmacokinetic studies showed that the absorption rate and elimination half-life were significantly prolonger, and the oral bioavailability had been improved when SAL was encapsulated in the water phase of nanoemulsion. Overall, the w/o nanoemulsion is a hopeful way to enhance oral absorption of the drug with polyphenols. It can be effectively delivered via the oral route.

References

[1] Panossian A, Wikman G, Sarris J. Rosenroot (*Rhodiola rosea*): traditional use, chemical composition, pharmacology and clinical efficacy [J]. *Phytomedicine*, 2010, **17**(7): 481-493.

[2] Ju LJ, Wen XH, Wang CJ, *et al*. Salidroside, a natural antioxidant, improves beta-cell survival and function *via* activating AMPK pathway [J]. *Front Pharmacol*, 2017, **8**: 749.

[3] Zhu Y, Shi YP, Wu D, *et al*. Salidroside protects against hydrogen peroxide-induced injury in cardiac H9c2 cells *via* PI3K-Akt dependent pathway [J]. *DNA Cell Biol*, 2011, **30**(10): 809-819.

[4] Liu SS, Yu XW, Hu BJ, *et al*. Salidroside-rescued mice from experimental sepsis through anti-inflammatory and anti-apop-

tosis effects [J]. *J Surg Res*, 2015, **195**(1): 277-283.

[5] Li YH, Pham V, Bui M, *et al*. *Rhodiola rosea* L.: an herb with anti-stress, anti-aging, and immunostimulating properties for cancer chemoprevention [J]. *Curr Pharmacol Rep*, 2017, **3**(6): 384-395.

[6] Zhuang W, Yue LF, Dang XF, *et al*. Rosenroot (Rhodiola): potential applications in aging-related diseases [J]. *Aging Dis*, 2019, **10**(1): 134-146.

[7] Ma CY, Hu LM, Tao GJ, *et al*. An UPLC-MS-based metabolomics investigation on the anti-fatigue effect of salidroside in mice [J]. *J Pharm Biomed Anal*, 2015, **105**: 84-90.

[8] Fang DL, Chen Y, Xu B, *et al*. Development of lipid-shell and polymer core nanoparticles with water-soluble salidroside for anti-cancer therapy [J]. *Int J Mol Sci*, 2014, **15**(3): 3373-3388.

[9] Chiu TF, Chen LC, Su DH, *et al*. Rhodiola crenulata extract for prevention of acute mountain sickness: a randomized, double-blind, placebo-controlled, crossover trial [J]. *BMC Complement Altern Med*, 2013, **13**(1): 298.

[10] Nan JX, Jiang YZ, Park EJ, *et al*. Protective effect of *Rhodiola sachalinensis* extract on carbon tetrachloride-induced liver injury in rats [J]. *J Ethnopharmacol*, 2003, **84**: 143-148.

[11] Guo N, Ding WM, Wang Y, *et al*. An LC-MS/MS method for the determination of salidroside and its metabolite *p*-tyrosol in rat liver tissues [J]. *Pharm Biol*, 2014, **52**(5): 637-645.

[12] Petsalo A, Jalonen J, Tolonen A. Identification of flavonoids of *Rhodiola rosea* by liquid chromatography-tandem mass spectrometry [J]. *J Chromatogr A*, 2006, **1112**(1−2): 224-231.

[13] Heenatigala PG, Singh S, Ashby CR, *et al*. Pharmaceutical topical delivery of poorly soluble polyphenols: potential role in prevention and treatment of melanoma [J]. *AAPS Pharm Sci Tech*, 2019, **20**(6): 250.

[14] Elsheikh MA, Elnaggar YSR, Gohar EY, *et al*. Nanoemulsion liquid preconcentrates for raloxifene hydrochloride: optimization and *in vivo* appraisal [J]. *Int J Nanomed*, 2012, **7**: 3787-3802.

[15] Lawrence MJ, Gareth DR. Microemulsion-based media as novel drug delivery systems [J]. *Adv Drug Deliv Rev*, 2000, **45**: 89-121.

[16] Zhao JH, Ji L, Wang H, *et al*. Microemulsion-based novel transdermal delivery system of tetramethylpyrazine: preparation and evaluation *in vitro* and *in vivo* [J]. *Int J Nanomed*, 2011, **6**: 1611-1619.

[17] De Oca-Ávalos JMM, Candal RJ, Herrera ML. Nanoemulsions: stability and physical properties [J]. *Curr Opin Food Sci*, 2017, **16**: 1-6.

[18] Yukuyama MN, Kato ET, Lobenberg R, *et al*. Challenges and future prospects of nanoemulsion as a drug delivery system [J]. *Curr Pharm Des*, 2017, **23**(3): 495-508.

[19] Singh Y, Meher JG, Raval K, *et al*. Nanoemulsion: concepts, development and applications in drug delivery [J]. *J Control Release*, 2017, **252**: 28-49.

[20] Callender SP, Mathews JA, Katherine K, *et al*. Microemulsion utility in pharmaceuticals: implications for multi-drug delivery [J]. *Int J Pharm*, 2017, **526**(1−2): 425-442.

[21] Pineros I, Slowing K, Serrano DR, *et al*. Analgesic and anti-inflammatory controlled-released injectable microemulsion: Pseudo-ternary phase diagrams, *in vitro*, *ex vivo* and *in vivo* evaluation [J]. *Eur J Pharm Sci*, 2017, **101**: 220-227.

[22] Yukuyama M, Kato E, Araujo G, *et al*. Olive oil nanoemulsion preparation using high-pressure homogenization and D-phase emulsification–a design space approach [J]. *J Drug Deliv Sci Technol*, 2019, **49**: 622-631.

[23] Aboofazeli R, Lawrence M. Investigations into the formation and characterization of phospholipid microemulsions. I. Pseudo-ternary phase diagrams of systems containing water-lecithin-alcohol-isopropyl myristate [J]. *Int J Pharm*, 1993, **93**: 161-175.

[24] Palanuwech J, Potineni R, Roberts RF, *et al*. A method to determine free fat in emulsions [J]. *Food Hydrocoll*, 2003, **17**: 55-62.

[25] Elnaggar YSR, El-Massik MA, Abdallah OY. Fabrication, appraisal, and transdermal permeation of sildenafil citrate-loaded nanostructured lipid carriers versus solid lipid nanoparticles [J]. *Int J Nanomed*, 2011, **6**: 3195-3205.

[26] Yang MM, Chen T, Wang LC, *et al*. High dispersed phytophospholipid complex/TPGS 1000 with mesoporous silica to enhance oral bioavailability of tanshinol [J]. *Colloids Surf B Biointerfaces*, 2018, **170**: 187-193.

[27] Liu ZD, Zhang Q, Ding LL, *et al*. Preparation procedure and pharmacokinetic study of water-in-oil nanoemulsion of *Panax notoginseng* saponins for improving the oral bioavailability [J]. *Curr Drug Deliv*, 2016, **13**: 600-610.

[28] Alany RG, Rades T, Kustrin SA, *et al*. Effects of alcohols and diols on the phase behaviour of quaternary systems [J]. *Int J Pharm*, 2000, **196**: 141-145.

[29] Li WH, He Y. Preparation and intestinal absorption effect of 5-fluorouracil microemulsion in rats [J]. *China Pharm*, 2008, **19**(7): 501-503.

[30] Sunazuka Y, Ueda K, Higashi K, *et al*. Combined effects of the drug distribution and mucus diffusion properties of self-microemulsifying drug delivery systems on the oral absorption of fenofibrate [J]. *Int J Pharm*, 2018, **546**(1−2): 263-271.

[31] Shinde UA, Modani SH, Singh KH. Design and development of repaglinide microemulsion gel for transdermal delivery [J]. *AAPS Pharm Sci Tech*, 2018, **19**(1): 315-325.

[32] Kogan A, Garti N. Microemulsions as transdermal drug delivery vehicles [J]. *Adv Colloid Interfac Sci*, 2006, **123−126**: 369-385.

[33] Rashid MA, Naz T, Abbas M, *et al*. Chloramphenicol loaded microemulsions: development, characterization and stability [J]. *Colloid Interfac Sci Commun*, 2019, **28**: 41-48.

[34] Wantida C, Thomas R, Siriporn O. Characterization and *in vitro* permeation study of microemulsions and liquid crystalline systems containing the anticholinesterase alkaloidal extract from *Tabernaemontana divaricate* [J]. *Int J Pharm*, 2013, **452**(1−2): 201-210.

[35] Alany RG, Tucker IG, Davies NM, *et al*. Characterizing colloidal structures of pseudo ternary phase diagrams formed by oil/water/amphiphile systems [J]. *Drug Dev Ind Pharm*, 2001, **27**(1): 31-38.

[36] Zhang J, Michniak-Kohn B. Investigation of microemulsion

microstructures and their relationship to transdermal permeation of model drugs: Ketoprofen, lidocaine, and caffeine [J]. *Int J Pharm*, 2011, **421**(1): 34-44.

[37] Li JW, Guo XJ, Liu ZD, *et al*. Preparation and evaluation of charged solid lipid nanoparticles of tetrandrine for ocular drug delivery system: pharmacokinetics, cytotoxicity and cellular uptake studies [J]. *Drug Dev Ind Pharm*, 2014, **40**(7): 980-987.

[38] Etman SM, Elnaggar YSR, Abdelmonsif DA, *et al*. Oral brain-targeted microemulsion for enhanced piperine delivery in Alzheimer's disease therapy: *in vitro* appraisal, *in vivo* activity, and nanotoxicity [J]. *AAPS Pharm Sci Tech*, 2018, **19**(8): 3698-3711.

[39] Godfrey KR, Arundel PA, Dong ZM, *et al*. Modelling the double peak phenomenon in pharmacokinetics [J]. *Comput Meth Prog Biomed*, 2011, **104**(2): 62-69.

[40] Ogungbenro K, Pertinez H, Aarons L. Empirical and semi-mechanistic modelling of double-peaked pharmacokinetic profile phenomenon due to gastric emptying [J]. *AAPS J*, 2015, **17**(1): 227-236.

[41] Qi DL, Yang XL, Chen J, *et al*. Determination of chikusetsusaponin V and chikusetsusaponin IV in rat plasma by liquid chromatography-mass spectrometry and its application to a preliminary pharmacokinetic study [J]. *Biomed Chromatogr*, 2013, **27**(11): 1568-1573.

[42] Luo YF, Chen DW, Ren LX, *et al*. Solid lipid nanoparticles for enhancing vinpocetine's oral bioavailability [J]. *J Contr Release*, 2006, **114**(1): 53-59.

[43] Vasir JK, Tambwekar K, Garg S. Bioadhesive microspheres as a controlled drug delivery system [J]. *Int J Pharm*, 2003, **255**(1−2): 13-32.

[44] Tran TH, Ramasamy T, Truong DH, *et al*. Preparation and characterization of fenofibrate-loaded nanostructured lipid carriers for oral bioavailability enhancement [J]. *AAPS Pharm Sci Tech*, 2014, **15**(6): 1509-1515.

Cite this article as: LIANG Chun-Xia, QI Dong-Li, ZHANG Li-Na, LU Peng, LIU Zhi-Dong. Preparation and evaluation of a water-in-oil nanoemulsion drug delivery system loaded with salidroside [J]. *Chin J Nat Med*, 2021, **19**(3): 231-240.